Carbon 183 (2021) 380–389

Contents lists available at ScienceDirect

Carbon

journal homepage: www.elsevier.com/locate/carbon

Research Article

Temperature dependence of water cluster on functionalized graphite

Toshihide Horikawa [a, *], Ryuto Yuasa [a], Ken Yoshida [a], D.D. Do [b]

[a] Graduate School of Technology, Industrial and Social Sciences, University of Tokushima, 2-1 Minamijosanjima, Tokushima, 770-8506, Japan
[b] School of Chemical Engineering, University of Queensland, St. Lucia, QLD, 072, Australia

ARTICLE INFO

Article history:
Received 5 April 2021
Received in revised form
17 June 2021
Accepted 7 July 2021
Available online 10 July 2021

Keywords:
Water adsorption
Water cluster formation
Temperature dependence
Functionalized graphite

ABSTRACT

Our recent experimental study of water adsorption in micro-mesoporous carbons at 263 K and 298 K show an unusual temperature dependence of adsorbed density with higher loading at 298 K at the same reduced pressure. The difference is in the filling of mesopore at 298 K and its absence at 263 K, and it was conjectured to the growth of water clusters on the functional groups in the confined space of mesopores in which the water clusters at 298 K are sufficiently large to induce the subsequent filling. Since the growth of these clusters and their coalescence is the prerequisite for filling, the filling is absent at 263 K simply because of the smaller size of the clusters, preventing them from coalescence and hence, no filling. In a quest to understand the effects of temperature on water adsorption in micro-mesoporous carbon, we used molecular dynamic simulation to reveal the mechanism of water adsorption around functional groups from 263 K to 328 K to clarify the growth of the water cluster as a function of temperature. The results clearly show that the water cluster is larger at 298 K compared to 263 K, confirming the conjecture from our previous works.

1. Introduction

Water is indispensable in our lives, and we are fortunate that it is abundant on our planet. One of the reasons for its importance is its high dipole moment, for which the interaction between water molecules is so strong to the extent that the term “hydrogen bonding” is reserved for water and other associating fluids, such as ammonia and methanol. Despite the simplicity of water molecules with three atoms and their respective partial charges, the interaction via hydrogen bonding is interesting, because of the directional “bonding” between the oxygen atom of one water molecule and the hydrogen atom of a neighboring molecule. The strength of this “bonding” is due to the small size of the hydrogen atom for which its positive partial charge is closely approached by the negative partial charge on the oxygen atom, resulting in a very strong electrostatic interaction to the extent that it is regarded as “bonding” although there is no bond in its very strict sense. The interaction between water and surfaces carrying charges also has the same feature of directional interaction, once again due to the small size of the hydrogen atom. This means that any functional group that is attached to a solid surface has an accessible partial charge (for example the oxygen atom on the carboxy group) can readily form a hydrogen bonding with a partial charge of opposite sign on the water molecule. It is due to this hydrogen bonding, not just in the intermolecular interaction of water but also between water and functional groups on the solid surface, that adsorption of water depends on the relative strength between these interactions.

It is important for scientists and engineers to understand the specific role of water in different scientific disciplines, including chemistry, biology, geology, nanotechnology, and materials technology. In industrial separation and purification processes with porous materials, one of the major problems is associated with mixtures containing water because the presence of water can severely reduce the capacity of contaminants that are desired to be removed. One logical solution to this is to choose hydrophobic solids, such as “perfect” graphite or porous carbon with perfect graphene pore walls; however, no such ideal solid exists because porous carbons, such as activated carbon, always contain a small residue of functional groups that induces the nucleation of water clusters and the subsequent penetration of water into the confined space of micropores, resulting in a significant reduction of the volume space for the removal of contaminants. Therefore, for the successful utilization of carbon adsorbents, it is important to understand at a fundamental level how water molecules interact with functional groups as this is the first step in a sequence of processes for water adsorption. Without this step, water does not adsorb on

* Corresponding author.
E-mail address: horikawa@tokushima-u.ac.jp (T. Horikawa).

https://doi.org/10.1016/j.carbon.2021.07.024

the surface of graphene because the intermolecular interaction of water is much stronger than the water-graphene interaction. Fundamental insight can be gained by carrying out water adsorption at very low loadings, where the intrinsic interaction between a water molecule and a functional group can be analyzed and quantified [1–5].

Adsorption on carbons has a very long history of more than 200 years with numerous publications on adsorption of a wide range of adsorbates in carbons of different pore structures and surface chemistry [6–16]. The complexity and the interplay between many parameters of adsorbate/adsorbent pair make it impossible to delineate the effects of each parameter, and to this end, computer simulation has been increasingly used to understand water adsorption at the microscopic level, and simulation results have shed greater light on the mechanism of water adsorption on carbons [4,5,17–33]. Recently, we reported simulation and experimental results for water adsorption on graphite, microporous carbons, and mesoporous carbons [1,2,[10]17,29–31,33], and the previous results can be interpreted based on the scenario in which water adsorbs initially on functional groups to form embryos of a few water molecules, which act as nucleation sites for further water molecules to attach to form clusters which then grow in size with pressure. The initiation of the embryo around the functional groups is due to the strength of the water-functional group is comparable to the intermolecular interaction of water, which is, in turn, stronger than the interaction between water and graphene [1,2,5,17,29].

In a recent report on water adsorption in microporous and mesoporous carbons, we theoretically explained the adsorption mechanism that the formation of water cluster and its growth with pressure is very important and this cluster needs to reach a certain size before water can fill the confined space of pores and this critical size is pore-size dependent [10]. Perhaps, the most striking finding in our recent experimental work on water adsorption on nonporous graphite, micro-mesoporous carbons is the unusual temperature dependence of the adsorption isotherm, in that the adsorbed density is higher with increasing temperature [8,29]. For purely microporous carbons isotherms exhibit only one step of uptake for temperatures between 263 K and 298 K, and the reduced pressure for this uptake is independent of temperature [8]. On the other hand, isotherms at 298 K for porous carbons whose pore size distributions have distinct peaks for the micropore and mesopore range show a two-step uptake, while those at 263 K exhibit only one-step uptake, which is practically the same as the first step of the 298 K isotherm of microporous carbons when they are plotted against the reduced pressure. We attributed that the first and second steps are due to water filling in micropores and mesopores, respectively, and conjectured that this unusual temperature dependence on water adsorption is associated with the temperature dependence of the cluster size [8,29]. Therefore, the objective of this paper is to elucidate this unusual temperature dependence by investigating the microscopic behavior of water clusters on functionalized graphite with molecular dynamics (MD) simulation.

2. Simulation methods

2.1. Interaction models

Water molecule is modeled by the simple-point charge model (SPC) [34,35]. The molecular parameters for the functional groups are taken from the all-atom optimized potentials (OPLS-AA) force fields [28]. The values of the potential parameters are summarized in Table 1. The functionalized graphite was modeled by stacking three graphene layers in the ABA configuration and the uppermost graphene layer is grafted with either one or two functional groups (carboxy and hydroxy) positioned at the lattice points of graphene. In the case of two functional groups, we used three different spacings 0.984, 1.968, and 2.952 nm (Fig. 1). The dimensions of each graphene layer are 9.963 nm × 10.08 nm, and the interlayer spacing between adjacent graphene layers is 0.335 nm (Fig. 2).

Table 1
The molecular parameters of MD simulation.

name	site	σ [nm]	ε [kJ/mol]	q [e]	geometry
H_2O(SPC) [a]	O	0.3166	0.6502	−0.82	$l_{O\text{-}H} = 0.1$ nm
	H			0.41	$\angle_{HOH} = 109.47°$
carboxy [b]	C	0.3500	0.2761	0.08	$l_{C\text{-}C} = 0.152$ nm
	C(COOH)	0.3750	0.4393	0.55	$l_{C=O} = 0.1214$ nm
	O (=O)	0.2960	0.8786	−0.50	$l_{C\text{-}O} = 0.1364$ nm
	O (−H)	0.3000	0.7113	−0.58	$l_{O\text{-}H} = 0.097$ nm
	H			0.45	$\angle_{CCO} = 111°$
					$\angle_{OCO} = 123°$
					$\angle_{COH} = 107°$
hydroxy [b]	C	0.3550	0.2929	0.20	$l_{C\text{-}O} = 0.1364$ nm
	O	0.3070	0.7113	−0.64	$l_{O\text{-}H} = 0.096$ nm
	H	0.2420	0.1255	0.44	$\angle_{COH} = 110.5°$

[a] The simple-point charge model [34,35].
[b] The parameters are from OPLS-AA force fields [28].

Molecular dynamic simulations were performed in the canonical (*NVT*) ensemble (constant number of molecules, volume, and temperature) using the open-source code GROMACS package 2018.6 (released Feb. 22, 2019). The intermolecular potential energy is calculated as the sum of pair-wise energies of Lennard-Jones (LJ) interaction and Coulombic interaction and Lorentz-Berthelot mixing rules were used to calculate the cross parameters. LJ and electrostatic interaction energies were calculated with a cut off radius of 0.950 nm (three times the collision diameter of the oxygen atom in the SPC model). Long-range electrostatic interactions were accounted for with the Ewald summation method using particle mesh Ewald for the reciprocal part [36]. The constant temperature was achieved by rescaling velocities at an interval of 1 ps.

The dimensions of the simulation box are 10.086 nm × 10.222 nm × L_z (Fig. 3), where L_z is set to be 620–680 nm; exact values are shown in Table 2. The functionalized graphite was placed at the bottom of the simulation box and the position of all the constituent aromatic carbon atoms are completely fixed (i.e. the carbon atoms do not have any vibration or displacement) during the course of the simulation, except for the atoms of the functional groups that are subject to the law of motion. For each temperature, the number of molecules introduced into the box was adjusted (at the end of every 20 ns) using the equation of states for the perfect gas so that the time averaged pressure at equilibrium is the same as the bulk saturation pressure, or sublimation pressure, P_0, except for $T = 263$ K where the system is equilibrated at a pressure of twice P_0 because the saturated vapor pressure is very low. We employed the experimental P_0 for the present MD simulation because the saturation pressures of SPC are not available in the low temperature range examined here; the P_0 values are listed in Table 2 for the temperatures studied in this work. The SPC model reproduces the experimental saturation pressures relatively well; the deviation from the experimental values at 373–523 K is within ~20%, which is much smaller than, for example, ~50% deviation for the SPC/E model [37].

The system was allowed to relax to equilibrium for a duration of 20 ps, beyond which we carried out simulations for the next 20 ns for the data sampling. The time step of the MD calculation was set to 1 fs and the data was collected every 1 ps. Periodic boundary conditions were employed in all three directions.

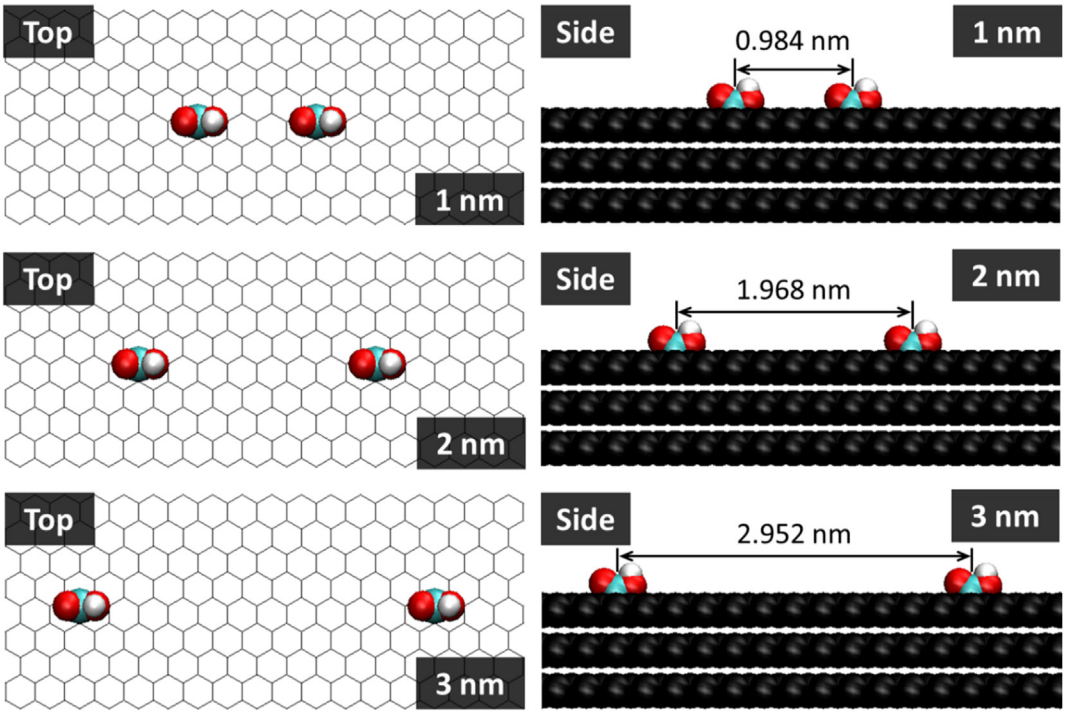

Fig. 1. Schematic of the graphite model with two functional groups grafted on the surface. The left panel is the top view and the right panel is the side view. (A colour version of this figure can be viewed online.)

2.2. Cluster size analysis

In this study, the size of the water cluster around the functional group was estimated by the distance from the functional group and the most distant water molecule from the functional group as a rough measure of the dimension of the cluster. The distance between the functional group and the outermost water was calculated from the number of water molecules in the cluster and the instantaneous radial distribution function (RDF) between water and the functional group; employing the RDF of the centers of mass of water and the functional group as the molecule-residue RDF. The position of the outermost water molecule is obtained as the value of radius where the hydration number obtained by the cumulative water-residue RDF attains the number of the water molecule in the cluster. The instantaneous RDF is obtained from the 10 frames, taken at an interval of 1 ps, at the end of every 10 ps. The instantaneous cluster size values at the time when the vapor pressure is equal to P_0 are collected to the different more than 100 points and used for the analysis described below.

3. Results and discussion

3.1. Cluster formation on a functional group

3.1.1. Carboxy group

We began our investigation with the simulation of water adsorption at 298 K on graphite with one carboxy group grafted at the center of the uppermost graphene layer. The simulation results for 50 water molecules are shown in Mov. 1 at the saturation pressure (supplementary material). It is observed that at this ambient temperature water molecules in the cluster constantly move around the functional group in synchronization with the rotation of the C–C sigma bond in the carboxy group to maintain their interactions with the carboxy group. The term cluster is defined loosely as a group of more than one water molecule connected via hydrogen bonding. The first water molecule approaches the carboxy group at 1.940 ns and the hydrogen bonding is realized via the strong electrostatic interaction between the partial charge on the water molecule and the partial charge of the opposite sign on the carboxy group. Because of the elongated carboxy with bearing positive partial charges on C- and H-atoms and negative partial charges on the two O-atoms, two modes of hydrogen bonding can be realized between water and carboxy group: one is between the O-atom of one water molecule interacting with the H-atom of the carboxy group and the other is between the H-atom of the water molecule and the O-atom of the carboxy group. Because of the many possible relative orientations between water molecules and the carboxy group, there are many possible interactions between water and carboxy group to form a dynamically evolving cluster: (1) one water is directly interacting with the carboxy group, and additional water molecules are attached to this water to form a string structure, (2) two water molecules directly interacting with the carboxy group and they are interacting either between themselves or with additional molecules in between. These two basic cluster configurations are dynamically interchanged by way of detachment and reattachment of water molecules. Other configurations are also possible, for example, a group of hydrogen bonded water molecules is attached to the end of the string configuration. The cluster can take diverse configuration owing to not only the small size of the hydrogen atom of the carboxy group but also it is positioned sufficiently distant from the graphene layer so that repulsion is avoided between water molecules and the uppermost graphene layer, allowing them to orient themselves to maximize the number of water molecules in the cluster. As we have stated in the introduction there is no bond formation in this hydrogen bonding, and this terminology could mislead some readers as the formation of a bond. It is to be noted here that a better term to describe this phenomenon is “strong attachment” rather than “adsorption” although the latter is often used in the literature. In a strict sense, adsorption would imply

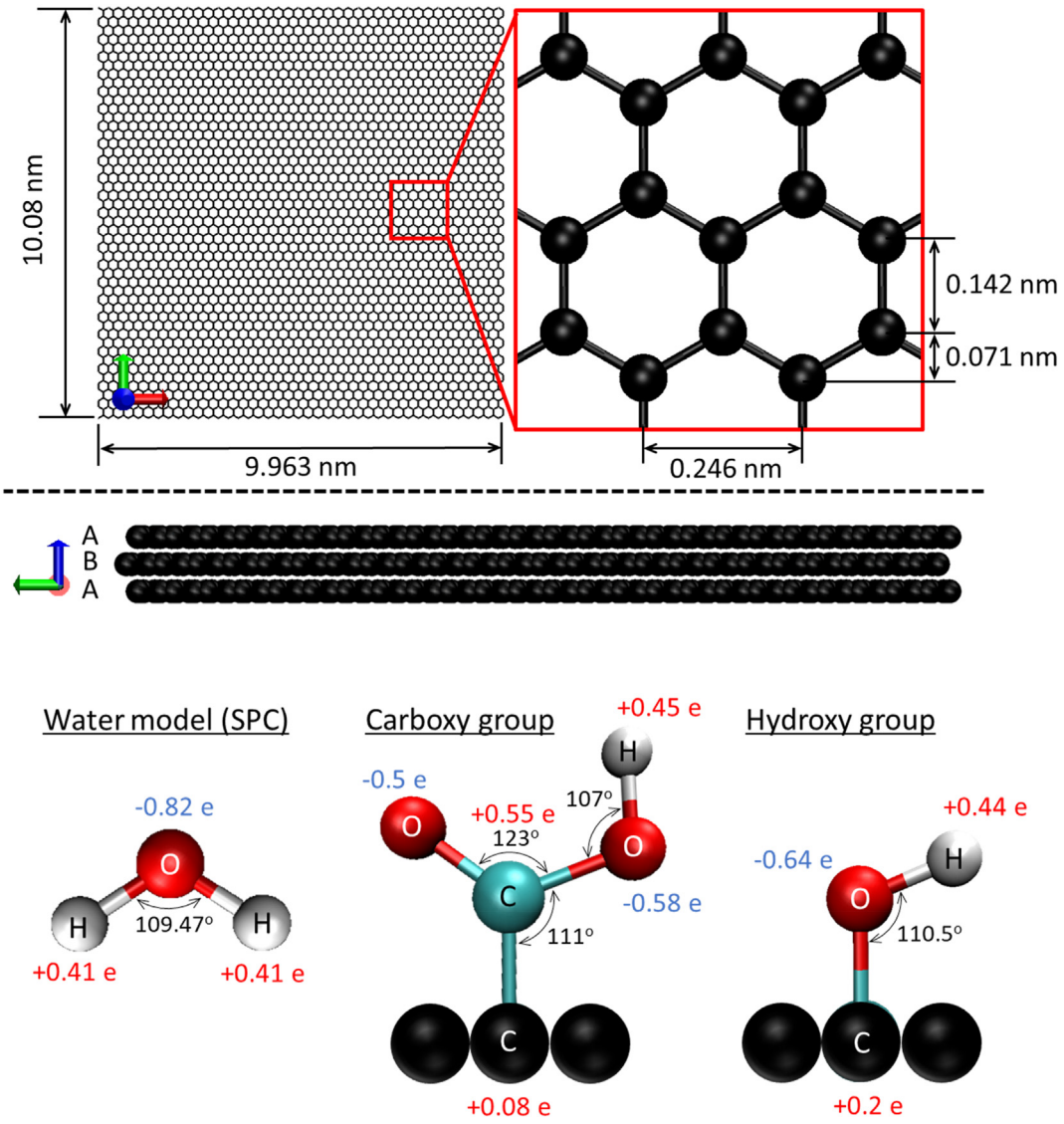

Fig. 2. Schematic of the graphite structure, water molecule, carboxy and hydroxy groups. (A colour version of this figure can be viewed online.)

attachment of a molecule on a mesoscopic surface whose dimension is greater than the molecular size of the adsorbate. However, to keep the traditional use of the term "hydrogen bonding" that is widely used in the literature, we continue to use it for the rest of this paper. Once the hydrogen bonding has occurred with the first water molecule, the second water approaches, and forms a hydrogen bond with this water/carboxy composite. Among all possible configurations of water clusters, the maximum size of the cluster of 11 molecules, having a string configuration, is 1.57 nm, measured from the reference point to the opposite end of the cluster. As the number of molecules in a cluster and its configuration are constantly changing, it is not possible to categorize the shapes of the cluster and assign a shape for each transient cluster. Since the number of molecules at the saturation pressure is finite it is clear that one functional group is not enough for the cluster to grow large enough for coalescing with neighboring clusters unless the separation distance between functional groups is less than twice the cluster size. Only when coalescence occurs and the confined space is small enough, for example, micropores and small mesopores, water can fill the volume of the confined space at a pressure less than the saturation pressure.

Supplementary video related to this article can be found at https://doi.org/10.1016/j.carbon.2021.07.024.

The above explanation for the nucleation of a cluster and its subsequent growth generally applies to all temperatures as well. The only difference is in the number of molecules involved in the cluster and its size at $P/P_0 = 1$. More details on the phenomenon of coalescence are given in Section 3.2 where we discuss the presence of two functional groups grafted on the surface.

3.1.2. Hydroxy group

For a hydroxy group grafted on the graphite surface, the formation of cluster and its growth are essentially the same as that for carboxy, but the detachment of water molecules from the cluster is more frequent because of the weaker electrostatic interactions, compared to the carboxy group (Mov. 2). This is simply because not only there are more partial charges on the carboxy group but its O–H group is more distant from the uppermost graphene layer than that of hydroxy, allowing water molecules more easily to adopt orientations favorable for the electrostatic interactions.

Supplementary video related to this article can be found at https://doi.org/10.1016/j.carbon.2021.07.024.

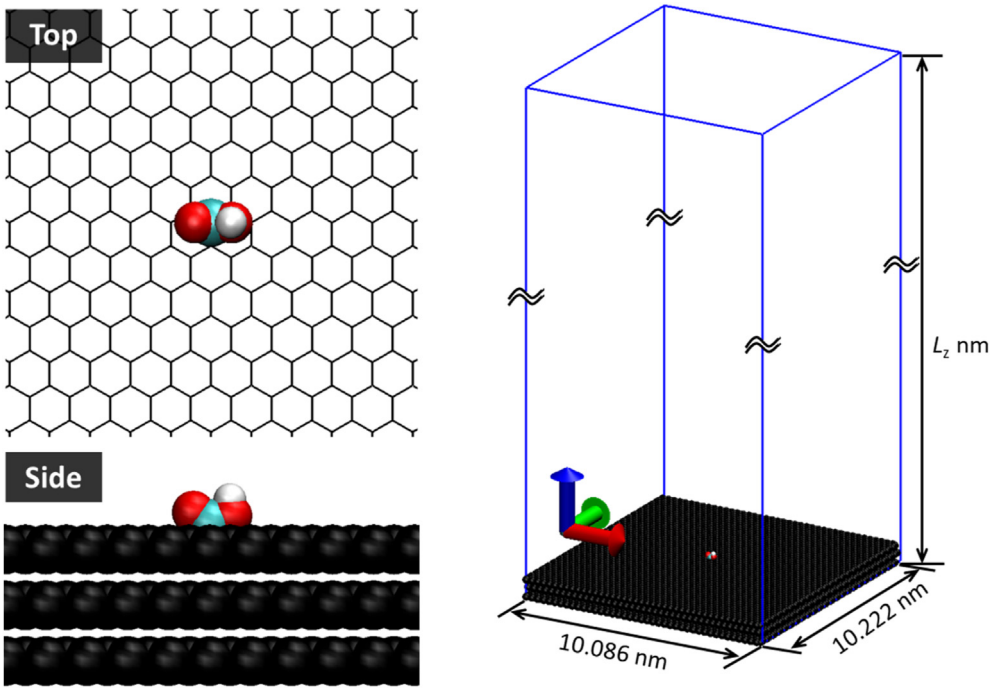

Fig. 3. Schematic of the graphite model with a functional group, and the simulation box with the graphite models. (A colour version of this figure can be viewed online.)

Table 2
The *height* of the simulation box and P_0 at each temperature.

Temperature [K]	263.15	283.15	298.15	313.15	328.15
L_Z **[nm]**	679.73	618.90	630.77	624.88	668.07
P_0 **[kPa]**	0.25985[a]	1.2282[b]	3.1699[b]	7.3849[b]	15.762[b]

[a] D.W. Green, R.H. Perry, "Perry's Chemical Engineers' Handbook, 8th ed.", McGraw-Hill (2007), pp. 2-48.
[b] NIST Chemistry Web Book.

3.1.3. Temperature dependence of water cluster

The snapshots of water molecules in a cluster localized around a carboxy group at $P/P_0 = 1$ for 263 K, 283 K, and 298 K, are shown in Fig. 4. The clusters in these snapshots show a string structure, which is a typical form among a variety of structures observed during the time course of adsorption. Surprisingly, the cluster size increases with increasing temperature from 263 K to 298 K. This is because of the smaller number of water molecules at 263 K and the greater thermal motions at 298 K. More interestingly, the increase in the cluster size with temperature reaches a plateau or even turns into a decrease for both carboxy and hydroxy groups when we raise the temperature above 298 K as can be seen in Fig. 5. The maximum for the cluster size at 298 K for both carboxy and hydroxy groups was analyzed using the least squares method, and we derived the slopes for three different ranges of the data points, e.g. 263–298 K, 283–313 K, and 298–328 K. It was found that the slopes change from positive to negative for both carboxy and hydroxy functional groups when the temperature crosses 298 K. The entropic factor comes into play for temperatures greater than 298 K, for which water molecules are distributed more on the graphite surface and also in the bulk gas phase. These results strongly substantiate the experimental data in our previous studies where we reported for the first time the unusual temperature dependence of the adsorbed density versus the reduced pressure on highly graphitized carbon, micro-, and mesoporous carbon, and mesoporous carbon with higher loading observed at 298 K compared to that at 263 K [8,29], and in the experimental data at high temperatures [38]. The number of molecules in the cluster decreases at high temperatures and this is indeed one of the factors that cause the decrease in the cluster size at higher temperatures. It is interesting to note that the decrease in the number of water molecules is significantly larger than that of the cluster size especially at 328 K. This means that the cluster can form a thinner and more elongated configuration at a higher temperature. This is probably because hydrogen bonds can be distorted or broken more frequently due to the greater thermal molecular motion and thus the exposure of the water cluster surface to the gas phase as well as to the graphite plane becomes more likely to occur. In other words, the weakening of the relative hydrophobicity of the vacuum as well as the graphite plane at high temperatures plays a role to disturb the compact aggregation of water molecules that prefer to form multiple hydrogen bonds and as a result, this effect can partially compensate the decrease in the number of water molecules in the cluster.

3.2. Cluster formation on two functional groups

Having discussed the behavior of water molecules in a cluster localized on one functional group, we now turn to the case of two functional groups to investigate possible synergetic interactions between water molecules and the functional groups. Let us first consider the case of a separation distance of 2 nm. Mov. 3 shows the MD simulation results for a duration of 3 ns for water interacting with two carboxy groups at the respective saturation pressures of 263 K, 298 K, and 328 K (supplementary materials). Even with the presence of a neighboring carboxy group, water molecules form a linear chain on each functional group, and the difference among the three temperatures is in the length of the cluster. At 263 K the cluster size is smaller than the separation distance, the two clusters behave independently from each other and as a result, they do not coalesce. However, for 298 K and 328 K, the clusters are large enough to induce the cross-hydrogen bonding aided by the rotation of the functional groups, resulting in the coalescence of the two clusters to form a fused cluster, which is constantly dissociated and

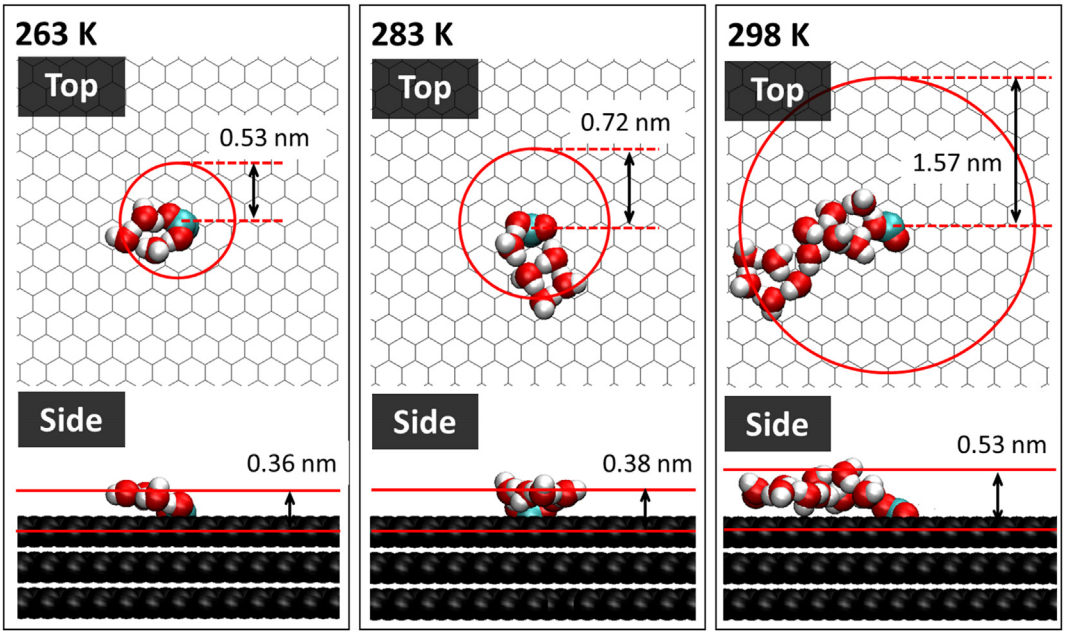

Fig. 4. Snapshots of the configurations for water adsorption on graphite surface with a carboxy group at $P/P_0 = 1$, and 263 K, 283 K, and 298 K. (A colour version of this figure can be viewed online.)

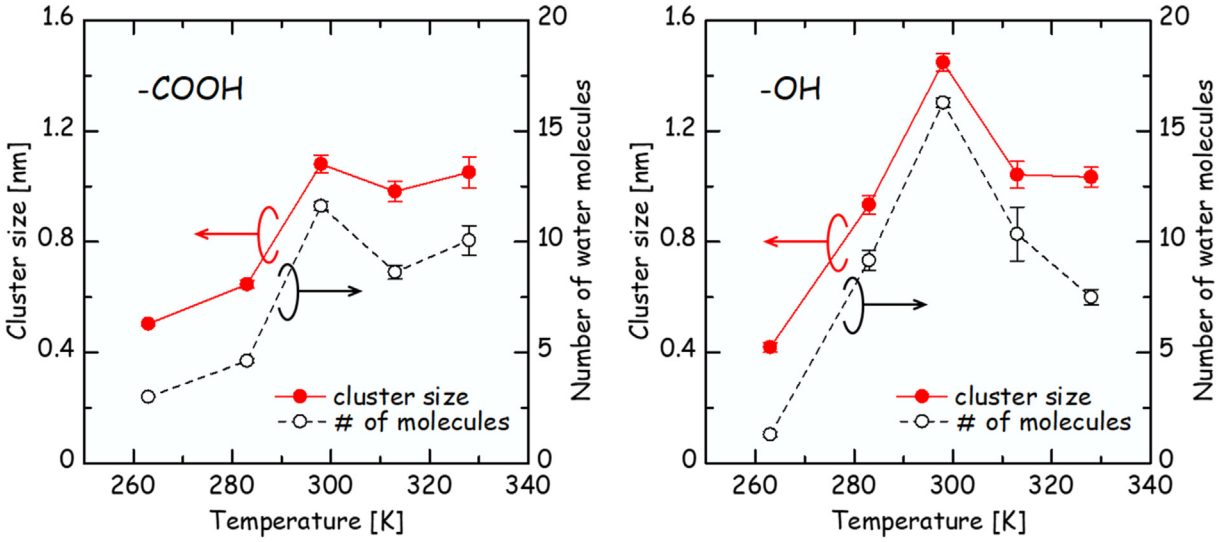

Fig. 5. Temperature dependence of the water cluster size and the number of water molecules in a cluster on carboxy group (LHS panel) and hydroxy group (RHS panel) at the saturation pressure. The error bars show 95% confidence intervals on the data of the cluster size, obtained from the sampling of more than 100 data points. (A colour version of this figure can be viewed online.)

reformed, due to the thermal motions of water molecules. The frequency of dissociation and reformation is greater for 328 K than 298 K, as physically expected.

Supplementary video related to this article can be found at https://doi.org/10.1016/j.carbon.2021.07.024.

The representative snapshots of water molecules in the clusters on two carboxy groups, separated by 1 nm, 2 nm, and 3 nm, at 263 K, 298 K, and 328 K are shown in Fig. 6. Also shown in the same figure is the 2D-density distributions of the center of mass of water molecule average over 1 ns For the short separation distance of 1 nm between the two carboxy groups, coalescence is observed for all temperatures, even at 263 K, and the fused cluster for 298 K has a hemispherical shape and its height is three times the molecular size of water. For the larger separation distances of 2 nm and 3 nm, the two clusters behave independently from each other at 263 K, and coalescence occurs for 298 K and 328 K with the fused cluster subject to dissociation and reformation, whose frequency is greater for 328 K, compared to 298 K, which is resulted from the greater thermal motions of water molecules and rotation of functional groups.

Since the snapshots merely show an instant configuration of water molecules, we present in Fig. 6b the 2D-density distribution to show the time-average behavior of water molecules. The region that water molecules spent major of the time during the course of adsorption is shown in red color while the rarefied region is shown with navy blue color. The 2D-density distribution depends on the

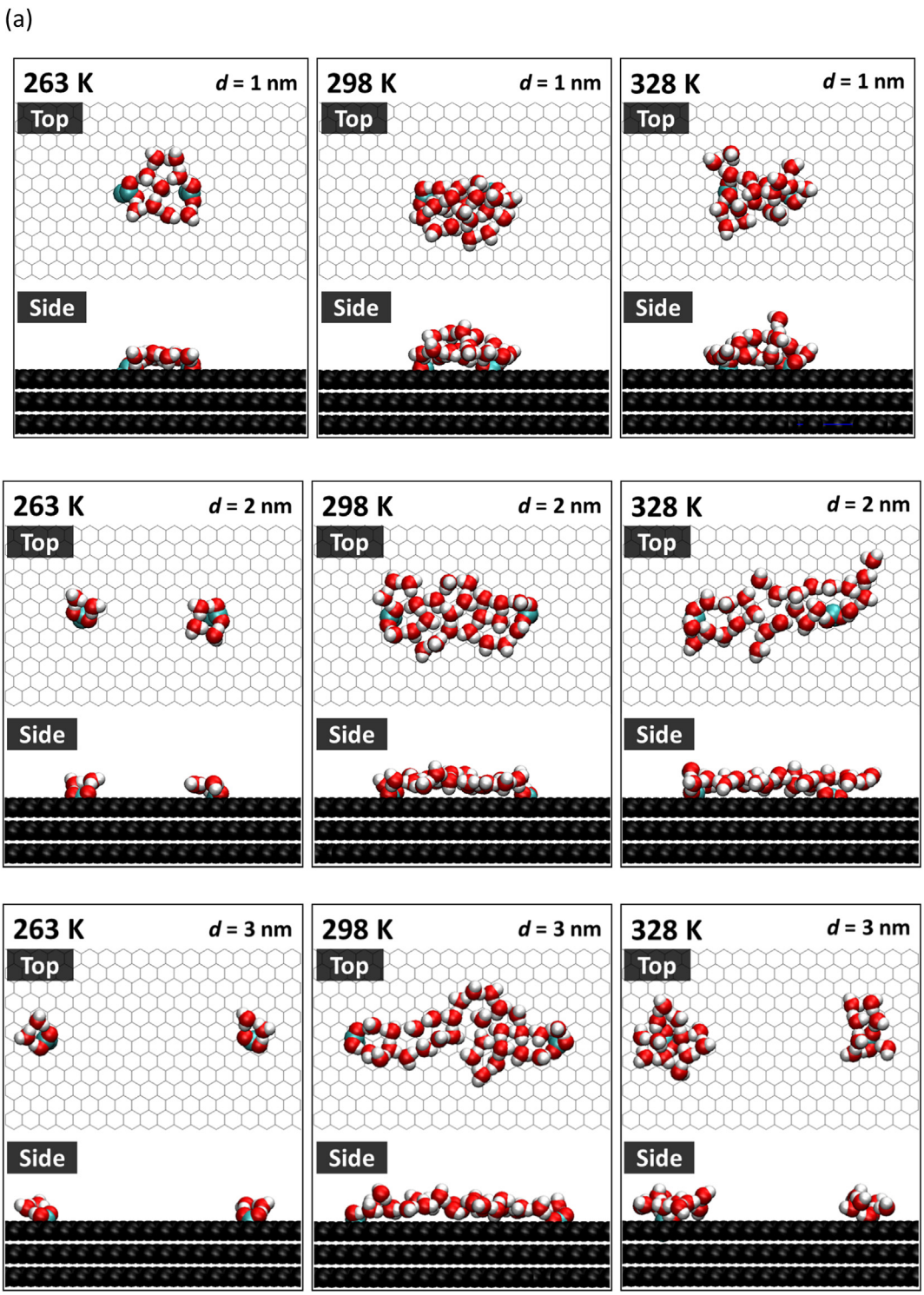

Fig. 6. (a) Snapshots of the configurations for water clusters on graphite surface with two carboxy groups which distances are 1 nm, 2 nm, and 3 nm at $P/P_0 = 1$, and 263 K, 298 K, and 328 K, and (b) its 2D-density distributions of water molecules for 1 ns. (c) Combined with snapshots and 2D-density distributions of the top of view. The reddish and blueish colors in the distribution indicate the higher and lower water density, respectively. (A colour version of this figure can be viewed online.)

separation distance between two functional groups and the temperature. For a separation distance of 1 nm, the fusion of the two clusters is observed over the entire temperature range examined as described above and thus the existence probability of water molecules is higher in between the two functional groups. The effect of the temperature variation is seen in the density distribution. The water molecules are the most highly localized within a limited area between the two functional groups at the lowest temperature of 263 K. At 298 K, the water density of the most concentrated region, shown in red color between the two functional groups, is

(b)

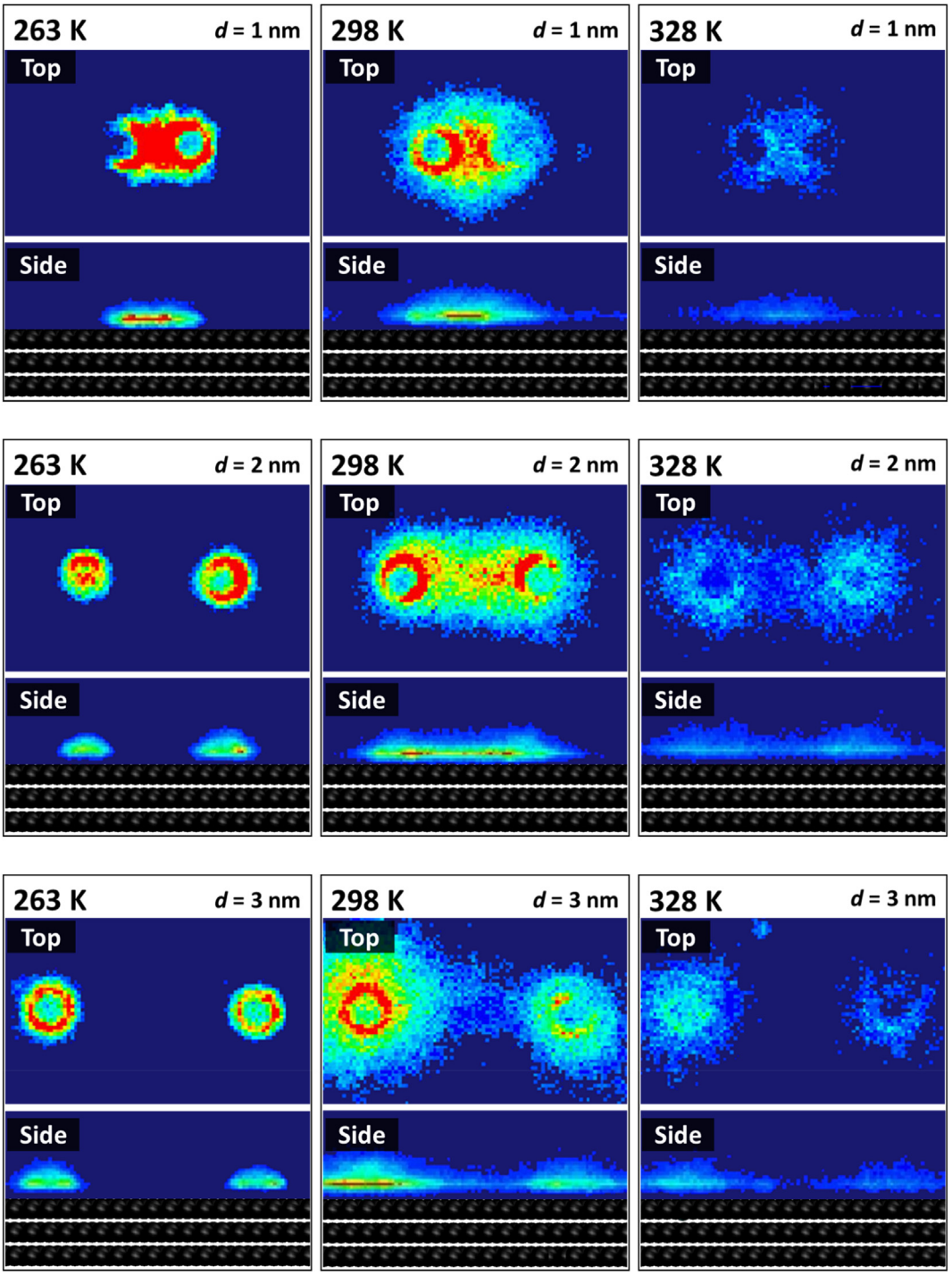

Fig. 6. (*continued*).

comparable to that at 263 K and the distribution of the medium density region spreads to the periphery of the fused clusters to surround the two functional groups. The total number of water molecules clustered around the functional groups, which corresponds to the integral of the distribution over the area occupied by the cluster, is larger at 298 K than that at 263 K because of the more frequent encounters of the gas-phase water molecules to the cluster on the graphene surface due to the higher saturation pressure and the resultant cluster size large enough to realize the cluster fusion. When the temperature is raised to 328 K, water molecules become further diffusive and spread over a wider range due to the enhanced thermal motions as well as the entropic factor. At 328 K, the thermal motions are greater, and the distribution becomes wider. As a result, the water density at its peak becomes smaller than that at 298 K, even with the higher saturation pressure at 328 K. The formation of the cluster is, therefore, less likely than that at 298 K because of the absence of the stable and concentrated aggregation of water molecules as a nucleus for the cluster growth.

Let us examine the water density distribution with larger functional-group separation distances of 2 nm and 3 nm. At 263 K, the two clusters are completely separated from each other for both 2 nm and 3 nm functional group separation. The temperature of 298 K is the most optimal temperature for the cluster formation due to the balance between hydrogen bonding formation and the vapor density as demonstrated above. At this temperature, there is seen the connection of the water distribution between the two clusters between the functional groups at 2 nm separation, and even at 3 nm separation, the two clusters are barely connected by a narrow bridging area. At 328 K, the water molecules are more dispersed the overall density distribution is lower and broader because water molecules readily detach from the cluster and translate to the surface of the graphene layer at this higher temperature. The clusters around the two functional groups are still connected at the separation distance of 2 nm, however, the density in the connection area is much lower than that at 298 K and is not sufficient for the clusters to maintain the long-lived fused cluster. At 3 nm separation of the functional groups, the two clusters are completely separated and there is almost no chance of the two clusters to contact each other.

In conclusion, 298 K is the suitable temperature for cluster formation and its stability and possible coalescence when the neighboring functional groups are apart within 2 nm. For temperatures below 298 K, the cluster formation remains but its size is smaller than at 298 K, making the coalescence is unlikely, unless the separation distances are less than 1 nm. On the other hand, for temperatures above 298 K, the thermal motions make the cluster less stable because of the high frequency of detachment of water molecules from the cluster.

4. Conclusions

We investigated the dynamic behavior of water adsorption on one or two functional groups, carboxy or hydroxy, using molecular dynamic simulation, with particular attention to the temperature dependence of the clusters and their possible coalescence. The first water molecule approaching the functional group forms hydrogen bonding via the strong electrostatic interaction between the partial charges on the water molecule and those on the functional group. Further approaching water molecules to the functional group formed a cluster that adopts different structures which dynamically interchanged because of the thermal motions of the water molecules and the rotation of the sigma bonds in the functional group. For the range of temperatures from 263 to 328 K, it was found that the cluster size at 263 K is the smallest, and it is largest at 298 K for either carboxy or hydroxy group. In the presence of two functional groups grafted on the surface, three spacings were investigated: 1, 2, and 3 nm. For 1 nm separation distance, the clusters on functional groups merge at all temperatures to form a fused cluster. However, for larger separation distances of 2 nm and 3 nm, the clusters on the functional groups behave independently, especially,

(c)

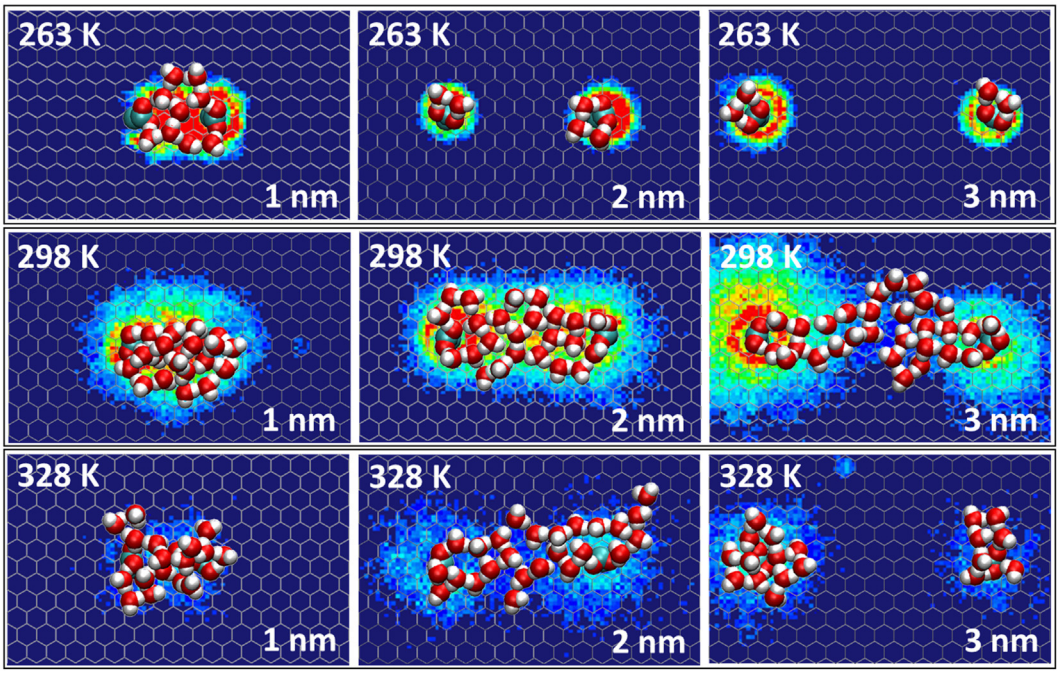

Fig. 6. (*continued*).

coalescence does not occur because of the small size of the clusters at 263 K. On the other hand, 298 K is found to be the suitable temperature for coalescence when the neighboring functional groups are less than 2 nm apart. For temperatures greater than 298 K, water molecules in the fused cluster readily detach at a higher frequency because of the greater thermal motions that make the cluster less stable. Our simulation results clearly show that the water cluster is larger at 298 K compared to 263 K, confirming the conjecture made in our previous works, and they shed great insight into the mechanism of the water cluster formation at different temperatures.

CRediT authorship contribution statement

Toshihide Horikawa: Conceptualization, Methodology, Investigation, Writing – original draft, Writing – review & editing, Supervision, Project administration, Funding acquisition. **Ryuto Yuasa:** Software, Validation, Investigation, Visualization. **Ken Yoshida:** Software, Validation. **D.D. Do:** Writing – review & editing, Supervision.

Declaration of competing interest

The authors declare that they have no known competing financial interests or personal relationships that could have appeared to influence the work reported in this paper.

Acknowledgement

This work was partially supported by the Japan Society for the Promotion of Science, Grant-in-Aid for Scientific Research(C) (JP19K05125). The computations were performed using Research Center for Computational Science, Okazaki, Japan.

References

[1] V.T. Nguyen, T. Horikawa, D.D. Do, D. Nicholson, On the relative strength of adsorption of gases on carbon surfaces with functional groups: fluid–fluid, fluid–graphite and fluid–functional group interactions, Carbon 61 (2013) 551–557.
[2] V.T. Nguyen, T. Horikawa, D.D. Do, D. Nicholson, Water as a potential molecular probe for functional groups on carbon surfaces, Carbon 67 (2014) 72–78.
[3] Y. Zeng, H. Xu, T. Horikawa, D.D. Do, D. Nicholson, Henry constant of water adsorption on functionalized graphite: importance of the potential models of water and functional group, J. Phys. Chem. C 122 (42) (2018) 24171–24181.
[4] L. Liu, S. Tan, T. Horikawa, D.D. Do, D. Nicholson, J. Liu, Water adsorption on carbon - a review, Adv. Colloid Interface Sci. 250 (2017) 64–78.
[5] Y. Zeng, L. Prasetyo, V.T. Nguyen, T. Horikawa, D.D. Do, D. Nicholson, Characterization of oxygen functional groups on carbon surfaces with water and methanol adsorption, Carbon 81 (2015) 447–457, 0.
[6] S. Kiefer, E. Robens, Some intriguing items in the history of volumetric and gravimetric adsorption measurements, J. Therm. Anal. Calorim. 94 (3) (2008) 613–618.
[7] T. Horikawa, N. Sakao, Ji Hayashi, D. Do, M. Katoh, K.-I. Sotowa, Preparation of nitrogen-doped porous carbon and its water adsorption behaviour, Adsorpt. Sci. Technol. 31 (2) (2013) 135–144.
[8] T. Horikawa, N. Sakao, D.D. Do, Effects of temperature on water adsorption on controlled microporous and mesoporous carbonaceous solids, Carbon 56 (2013) 183–192.
[9] T. Horikawa, N. Sakao, T. Sekida, Ji Hayashi, D.D. Do, M. Katoh, Preparation of nitrogen-doped porous carbon by ammonia gas treatment and the effects of N-doping on water adsorption, Carbon 50 (5) (2012) 1833–1842.
[10] T. Horikawa, T. Sekida, Ji Hayashi, M. Katoh, D.D. Do, A new adsorption-desorption model for water adsorption in porous carbons, Carbon 49 (2) (2011) 416–424.
[11] T. Horikawa, D.D. Do, D. Nicholson, Capillary condensation of adsorbates in porous materials, Adv. Colloid Interface Sci. 169 (1) (2011) 40–58.
[12] Y. Wang, P.T.M. Nguyen, N. Sakao, T. Horikawa, D.D. Do, K. Morishige, et al., Characterization of a new solid having graphitic hexagonal pores with a GCMC technique, J. Phys. Chem. C 115 (27) (2011) 13361–13372.
[13] T. Horikawa, Y. Kitakaze, T. Sekida, J. Hayashi, M. Katoh, Characteristics and humidity control capacity of activated carbon from bamboo, Bioresour. Technol. 101 (11) (2010) 3964–3969.
[14] K. Morishige, n-Propanol on graphite: the occurrence of two-dimensional smectic mesophase, J. Chem. Phys. 100 (4) (1994) 3252–3257.
[15] K. Morishige, N. Kawai, M. Shimizu, Occurrence of two-dimensional smectic liquid crystal in n-propanol adsorbed on graphite, Phys. Rev. Lett. 70 (25) (1993) 3904–3906.
[16] K. Morishige, K. Kawamura, M. Yamamoto, I. Ohfuji, Capillary condensation of Xe on exfoliated graphite, Langmuir 6 (8) (1990) 1417–1421.
[17] V.T. Nguyen, D.D. Do, D. Nicholson, A new molecular model for water adsorption on graphitized carbon black, Carbon 66 (2014) 629–636.
[18] T. Ohba, K. Kaneko, M. Endo, K. Hata, H. Kanoh, Rapid water transportation through narrow one-dimensional channels by restricted hydrogen bonds, Langmuir 29 (4) (2013) 1077–1082.
[19] A. Wongkoblap, D.D. Do, The effects of curvature and surface heterogeneity on the adsorption of water in finite length carbon nanopores: a computer simulation study, Mol. Phys. 106 (5) (2008) 627–641.
[20] A. Wongkoblap, D.D. Do, Adsorption of water in finite length carbon slit pore: comparison between computer simulation and experiment, J. Phys. Chem. B 111 (2007) 13949–13956.
[21] G. Birkett, D.D. Do, Simulation study of water adsorption on carbon black: the effect of graphite water interaction strength, J. Phys. Chem. 111 (15) (2007) 5735–5742.
[22] J.C. Liu, P.A. Monson, Monte Carlo simulation study of water adsorption in activated carbon, Ind. Eng. Chem. Res. 45 (16) (2006) 5649–5656.
[23] S. Picaud, B. Collignon, P.N.M. Hoang, J.C. Rayez, Molecular dynamics simulation study of water adsorption on hydroxylated graphite surfaces, J. Phys. Chem. B 110 (16) (2006) 8398–8408.
[24] A. Striolo, A.A. Chialvo, P.T. Cummings, K.E. Gubbins, Simulated water adsorption in chemically heterogeneous carbon nanotubes, J. Chem. Phys. 124 (7) (2006), 074710-11.
[25] A. Striolo, K.E. Gubbins, A.A. Chialvo, P.T. Cummings, Simulated water adsorption isotherms in carbon nanopores, Mol. Phys. 102 (3) (2004) 243–251.
[26] T. Ohba, H. Kanoh, K. Kaneko, Cluster-growth-induced water adsorption in hydrophobic carbon nanopores, J. Phys. Chem. B 108 (39) (2004) 14964–14969.
[27] A. Striolo, A.A. Chialvo, P.T. Cummings, K.E. Gubbins, Water adsorption in carbon-slit nanopores, Langmuir 19 (20) (2003) 8583–8591.
[28] M. Jorge, C. Schumacher, N.A. Seaton, Simulation study of the effect of the chemical heterogeneity of activated carbon on water adsorption, Langmuir 18 (24) (2002) 9296–9306.
[29] T. Horikawa, S. Tan, D.D. Do, K.-I. Sotowa, J.R. Alcántara-Avila, D. Nicholson, Temperature dependence of water adsorption on highly graphitized carbon black and highly ordered mesoporous carbon, Carbon 124 (2017) 271–280.
[30] T. Horikawa, M. Takenouchi, D.D. Do, K.-I. Sotowa, J.R. Alcántara-Avila, D. Nicholson, Adsorption of water and methanol on highly graphitized thermal carbon black and activated carbon fibre, Aust. J. Chem. 68 (9) (2015) 1336–1341.
[31] T. Horikawa, T. Muguruma, D.D. Do, K.-I. Sotowa, J.R. Alcántara-Avila, Scanning curves of water adsorption on graphitized thermal carbon black and ordered mesoporous carbon, Carbon 95 (2015) 137–143.
[32] K. Morishige, T. Kawai, S. Kittaka, Capillary condensation of water in mesoporous carbon, J. Phys. Chem. C 118 (9) (2014) 4664–4669.
[33] T. Horikawa, Y. Zeng, D.D. Do, K.-I. Sotowa, J.R. Alcántara Avila, On the isosteric heat of adsorption of non-polar and polar fluids on highly graphitized carbon black, J. Colloid Interface Sci. 439 (2015) 1–6, 0.
[34] H.J.C. Berendsen, J.P.M. Postma, W.F. van Gunsteren, J. Hermans, Interaction models for water in relation to protein hydration, in: B. Pullman (Ed.), Intermolecular Forces: Proceedings of the Fourteenth Jerusalem Symposium on Quantum Chemistry and Biochemistry Held in Jerusalem, Israel, April 13–16, 1981, Springer Netherlands, Dordrecht, 1981, pp. 331–342.
[35] H.J.C. Berendsen, J.R. Grigera, T.P. Straatsma, The missing term in effective pair potentials, J. Phys. Chem. B 91 (24) (1987) 6269–6271.
[36] U. Essmann, L. Perera, M.L. Berkowitz, T. Darden, H. Lee, L.G. Pedersen, A smooth particle mesh Ewald method, J. Chem. Phys. 103 (19) (1995) 8577–8593.
[37] G.C. Boulougouris, I.G. Economou, D.N. Theodorou, Engineering a molecular model for water phase equilibrium over a wide temperature range, J. Phys. Chem. B 102 (6) (1998) 1029–1035.
[38] T. Ohba, H. Kanoh, K. Kaneko, Affinity transformation from hydrophilicity to hydrophobicity of water molecules on the basis of adsorption of water in graphitic nanopores, J. Am. Chem. Soc. 126 (5) (2004) 1560–1562.